SYNTHESIS OF BaTiO₃ VIA MICROWAVE METHOD AND APPLICATION OF PANI/BaTiO₃ NANOCOMPOSITE AS COUNTER ELECTRODE IN HIGH PERFORMANCE DYE SENSITIZED SOLAR CELL

Recep Taş[*1] (iD) , *Mahir Gülen*[2] (iD)

[1]*Department of Biotechnology, Faculty of Science, Bartin University, 74100 Bartin, Turkey*
[2]*Department of Mechanical Engineering, Faculty of Engineering, Architecture and Design, Bartin University, 74100 Bartin, Turkey*

Abstract

Original scientific of paper

The development of the Dye sensitized Solar Cell (DSSC) architecture has opened the door to exciting new possibilities and photovoltaic (PV) systems to produce electricity at potentially lower costs. Therefore, DSSCs attract the attention of both researchers working in the energy field and the PV industry. Due to their low material cost, easy and inexpensive production processes and reasonable conversion efficiency, DSSCs are considered as an alternative to other conventional solar cells. In this work, BaTiO₃ nanoparticles were produced quickly and at low cost using the microwave method. Using the obtained BaTiO₃, Poly aniline (PANI)/BaTiO₃ nanocomposites were successfully sensitized and their usability as counter electrodes in DSSC was investigated. The coated PANI and nanocomposite films were characterized by Fourier-transform infrared spectroscopy (FT-IR), X-ray diffractometry (XRD), scanning electron microscopy (SEM), Cyclic Voltammetry (CV), and Electrochemical Impedance Spectroscopy (EIS) measurements. It was used as a counter electrode (CE) in DSSC architecture to characterize the photovoltaic potentials of the obtained nanocomposite films. In photovoltaic analysis, the conversion efficiency of DSSC using nanocomposite CE increased by 39% compared to cells employing pure PANI CE. As a result, it has been determined that synthesized nanocomposites can be used as CE in DSSCs instead of Pt, which is expensive and has limited stock in terms of both cost and durability and photovoltaic performance.

Keywords: Polyaniline, BaTiO₃, microwave method, nanocomposite, dye sensitized solar cell.

1   Introduction

Polymer and polymer-containing materials, which have an important place in our daily life, are widely used in industry and technology. The usefulness of some polymers with different structures and properties is related to the electrical properties of such materials, allowing them to be used in electrical insulators, dielectric capacitors or microwave devices. In addition, some polymers have superior optical properties, and these are the inner layers of aircraft windows, safety glass, etc. It is very important for areas [1].

On the other hand, depending on the increasing demands and the development of ceramic materials, the importance of dielectric characteristics (essentially insulating) is increasing day by day. At the same time, attempts to reduce the size of electronic devices such as expectations and communication tools are also inevitable. Along with these and similar reasons, studies have been intensifying in recent years on ceramic materials with high dielectric constant, such as BaTiO₃ [2].

The starting materials used in the production of advanced engineering ceramics are required to be submicron-sized, pure reactive and solidifiable at lower temperatures. At the same time, the importance of ceramics is increasing due to the rapid development of

electromagnetic devices with small sizes, which leading to high dielectric constant of a particle and low losses in microwave frequencies. Among the dielectric materials, BaTiO₃ is one of the most researched materials in terms of its high dielectric constant, low dielectric loss and high dielectric coefficient, resulting in high electric field [3, 4].

Among the conductive polymers, Polyaniline (PANI) is one of the most studied polymers due to its many superior properties. PANI is an unique conducting polymer whose properties not only depend on the oxidation state but also its protonation doping level and also on the nature of dopants [5]. These properties make the PANI a promising candidate for the fundamental study of potential device applications such as solar cells, light-emitting diodes, transparent electrodes, gas and humidity sensing, and many more in nanotechnology applications [6-8].

Many strategies have been developed to synthesize metal oxide structures, such as direct elemental reaction in a high temperature quartz tube [9], ball mill solid-state metathesis reaction [10], chemical vapor deposition [11], thermal decomposition [12], hydrothermal [13], solvothermal [14], sonochemical [15] and electrochemical [16]. However, many of these synthesis strategies have a lot of disadvantages that they require long time at high temperature or high-pressure conditions, complex

processes and advanced equipment or the technical skills required to prepare precursor materials. Whereas one of the ultimate goals in any scientific study is to find the simplest way to prepare the materials. From this point of view, the microwave method attracts attention due to its very fast synthesis of nanoscale metal oxide materials, high efficiency and environmental friendliness [17, 18]. Compared to traditional external heating methods, since microwave heating can provide rapid volumetric and homogeneous heating without heat conduction conditions, synthesis reactions can take place in a very short time [19]. The studies carried out show that microwave assisted synthesis is very simple, efficient and does not require extra annealing process, and especially its very short duration can reduce the cost of material synthesis and save time.

In this study, we report the synthesis of $BaTiO_3$ by microwave method and *in situ* synthesis of PANI/$BaTiO_3$ nanocomposites by chemical oxidation technique, and also employing PANI/$BaTiO_3$ nanocomposite films as counter electrode (CE) in DSSC architecture for the first time. The electrochemical features such as cyclic voltammetry (CV), Tafel polarization and electrochemical impedance spectroscopy (EIS), surface morphology and structural properties of pure PANI and PANI/$BaTiO_3$ nanocomposites films were investigated. In addition, the photovoltaic (PV) performance of DSSC employing the nanocomposite films as CE was investigated. Various PV parameters of the prepared DSSCs such as open-circuit voltage (V_{oc}), short circuit current density (J_{sc}), filling factor (FF), and overall efficiency were determined.

2   Materials and Methods

2.1 Chemicals

In the polymerization processes, aniline (Aldrich, 97%) was used as a monomer by distillation by distillation. Other chemicals used in the study were used without any processing, since they are of analytical purity. Distilled water (H_2O) and acetonitrile (Aldrich, 99.8%) were used as solvents, and ammonium persulfate ($NH_4S_2O_8$) (Sigma-Aldrich, 98%) was used as the raiser. Hydrochloric acid (HCl) (Sigma-Aldrich, 37%) was used as acid, and $TiCl_4$ (99.95%, Aldrich), $Ba(NO_3)_2$ (99%, Aldrich) were used in nanoparticle synthesis. To prepare photoanodes, Titanium (IV) oxide nanopowders (718467, Sigma Aldrich), di-tetrabutylammoniumcis-bis(isothiocyanato)bis(2,2'-bipyridyl-4,4'dicarboxylato)ruthenium(II) (N-719) dye (703214, Sigma Aldrich) were used. For syntesis of redox electrolyte; used iodine, 1–butyl–3–methylimidazolium iodide, 4–tert–butylpridine, lithium iodide hydrate and 3–methoxypropionitrile were used.

2.2 Synthesis of $BaTiO_3$ Nanoparticles

$BaTiO_3$ (BT) nanoparticles were synthesized using $TiCl_4$ (99.95%, Aldrich), $Ba(NO_3)_2$ (99%, Aldrich) in a 1:2 mixture of HCl:water. First, two solutions were prepared. In the first, 1 mL of $TiCl_4$ was slowly added to 25 mL of deionized water at 0 °C with stirring until it turned into a homogeneous solution. Second, similarly

0.88 g of $Ba(NO_3)_2$ was dissolved in 25 mL of deionized water. Then, these two solutions prepared were transferred to 25 mL of HCl:water mixture prepared at a ratio of 1:2 and mixed on magnetic stirrer for 30 minutes at 500 rpm stirring speed. The reaction mixture was placed in a 100 mL teflon autoclave, reaching 90% of its volume and providing maximum pressure efficiency. The pressure microwave autoclave was sealed and reacted for 10 min using 2.45 GHz of microwave radiation at a maximum power of 800 W. At this stage, the ambient temperature was measured as 140 °C. After the reaction, the autoclave was naturally cooled to room temperature. Thus, the solid product was washed several times with deionized water and alcohol, and then dried under vacuum at 80 ° C for 24 hours.

2.3 Synthesis of PANI/$BaTiO_3$ Nanocomposites

PANI/$BaTiO_3$ composites were synthesised *in situ* by adding $BaTiO_3$ to the medium at certain proportions during the oxidative polymerization of polyaniline. $BaTiO_3$ nano powders were dispersed in deionized water and mixed using magnetic stirrer at room temperature for 3 hours. In another beaker, a 1:1 ratio of aniline:HCl was mixed in acetonitrile at room temperature. Four of this PANI solution was prepared and $BaTiO_3$ was added in different proportions to three of these prepared PANI solutions. It was added from $NH_4S_2O_8$ solution to start polymerization. One pure PANI was synthesized. The solid product was washed several times with deionized water and acetonitrile and dried under vacuum at 60 °C for 12 hours. Obtained substances are named as in Table 1.

Table 1. The amount of PANI and $BaTiO_3$ by weight in the named samples.

Sample	% PANI	% BaTiO₃
SP	100	-
BP1	99,5	0,5
BP2	99	1
BP3	98	2

According to the FTIR results obtained in this study, the reaction scheme of the PANI/$BaTiO_3$ interaction can be considered as in Figure 1.
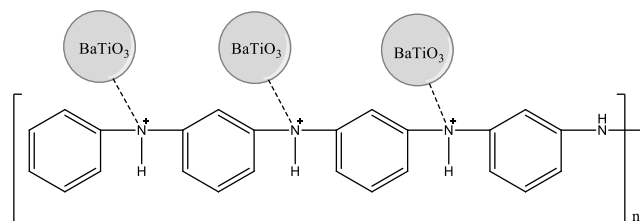
Figure 1. Predicted reaction scheme of BaTiO3 / PANI interaction.

2.4 Preparation of SP, BP1, BP2 and BP3 based CEs

The polymers SP, BP1, BP2, and BP3 were dissolved in formic acid at a certain concentration and then mixed with a magnetic stirrer for 2 hours. Before deposition, the fluorine-doped tin oxide (FTO) substrates (Asahi Glass;

sheet resistance: 15 Ω/cm2) were cleaned as reported in our previous study [20]. After cleaning, a spin coating was carried out to deposit polymer solutions on FTO substrates for 30 seconds at 2000 rpm. This process was repeated 15 times on each substrate to make the surface homogeneous. Lastly, SP, BP1, BP2, and BP3 catalyst-coated electrodes were annealed at 80 °C for 45 minutes.

2.5 Fabrication of DSSCs using SP, BP1, BP2 and BP3 based CEs

In the current study, titanium (IV) oxide based photoanodes were sensitized with 0.3 mM of di-tetrabutylammoniumcis-bis(isothiocyanato)bis(2,2'-bipyridyl-4,4'dicarboxylato)ruthenium(II) (N-719) dye overnight. The preperation of photoanodes was detailed in our previous reports [20]. Moreover, to prepare the I^{-3}/I^- redox electrolyte, 0.01 M iodine, 0.6 M 1–butyl–3–methylimidazolium iodide, 0.1 M 4–tert–butylpridine and 0.1 M lithium iodide hydrate were solved in 3–methoxypropionitrile, separately. Next, the solutions were poured in a bottle and mixed by magnetic stirrer for 5 h. Assembly of DSSCs was carried out by positioning the photoanode face up on a horizontal surface, and placing CE on top of the photoanode. The redox electrolyte was dropped at the edges of a electrode, and the electrolyte was drawn into the space between the photoanode and CE.

2.6 Characterizations

ATR-FTIR spectroscopy was used for the chemical characterization of the products obtained. The surface morphology of the samples was examined using the SEM (TESCAN, MAIA3 XM). X-ray diffraction spectra (XRD) of nanocomposites were examined with Rigaku D/MAX-2200 device with CuKα wavelength radiation beam at room temperature $10\ ° \leq 2\theta \leq 80\ °$. Cyclic voltametry (CV) and electrochemical impedence spectroscopy (EIS) measurements were done by a potentiostat/galvanostat instrument (ZİVE SP1). CV tests were conducted with three electrotes system; the nanocomposite CEs, platinum sheet and Ag/AgCl in 3 M NaCl were used as working electrode, counter electrode and reference electrode, respectively. CV of CEs was carried out in electrolytic medium containing 0.1 M LiClO₄, 0.1 M I^{-3}/I^- redox electrolyte and acetonitrile at scan rate of 50 mV s^{-1} and in range of -0.6–1.0 V. For EIS experiments, the symmetric cells were assembled with two identical CEs filled with the redox electrolyte of I^{-3}/I^-. The active area of the symmetric cells was 0.25 cm². In EIS analysis, the samples were scanned from 10 Hz to 100 kHz. The current density-potential (J-V) curves of prepared DSSCs were recorded using Fytronix PV characterization system under the AM 1.5 G illumination of 100 mW cm^{-2}.

3 Results and Discussion

FTIR spectra of polyaniline polymers doped with different proportions of BaTiO₃ are given in Figure 2. In the FT-IR spectrum of unoperated polyaniline, 1621 cm^{-1} and 1597 cm^{-1} NH₂ strain, 1492 cm^{-1} C-H bending, 1270

cm^{-1} C-N strain, 1171 cm^{-1} C-H bending and 744 cm^{-1} C-H strain characteristic peaks were observed. In the FT-IR spectrum of BaTiO₃ obtained by microwave method, characteristic peaks of BaTiO₃ resulting from 560 and 450 cm^{-1} Ti-O vibrations were observed. When the FT-IR spectra of composite samples are examined, the N-H stress peak seen in around 3300 cm^{-1} in polyaniline disappears in PANI/BaTiO₃ composite. This situation shows that the dominant interaction is between the H atoms in the N-H bond and the OH molecules in the solution environment, and it is bound to BaTiO₃ molecules through O atoms (Fig. 1).
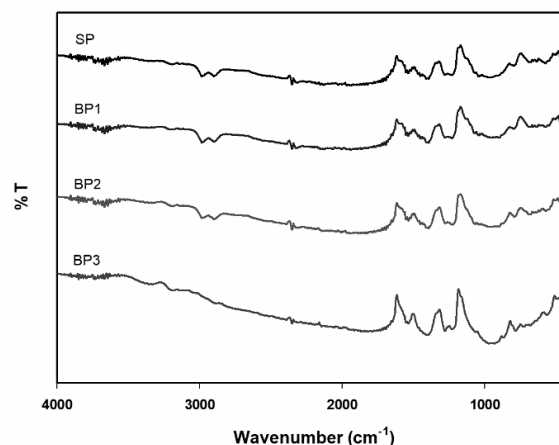

Figure 2. FTIR spectrums of SP, BP1, BP2, and BP3 nanocomposites, respectively.

XRD results of PANI composites prepared with BaTiO₃ obtained by microwave method are given in Figure 3. The $2\theta = 25.36°$ peak in the non-doped polymer is the main peak of polyaniline [21]. In addition, other peaks of pure polyaniline are seen at $2\theta = 21.08°$, 35.06°, and 64.92°. When the XRDs of composites are examined, the peaks of BaTiO₃ are clearly seen. As can be seen from Figure 3, natural orientation of crystal structure did not change, while the intensity of diffraction patterns of BaTiO₃ decreased slightly. This situation reveals that although PANI surrounds BaTiO₃ in composite formation, the crystal structure of BaTiO₃ does not change and it preserves its tetragonal perovskite structure.
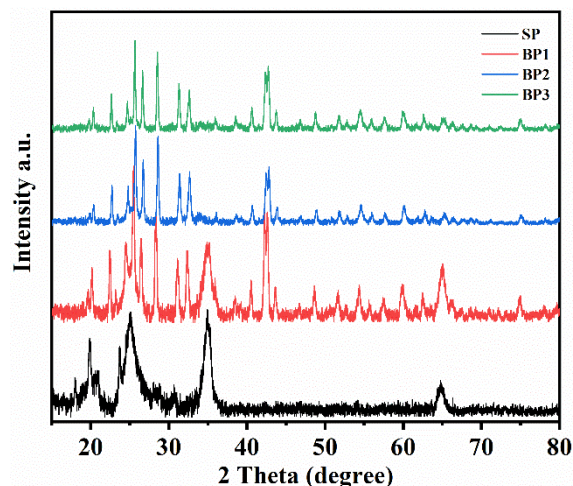

Figure 3. X-ray diffractogram patterns of SP, BP1, BP2, and BP3 nanocomposites, respectively.

In Figure 4, SEM images of the surface morphology of the composites where unadulterated polyaniline (Fig. 4a) and $BaTiO_3$ obtained by microwave method are doped at different proportions (Fig.4b-4d) are shown. In accordance with the XRD results, it is seen that the distribution of the $BaTiO_3$ in the polymer matrix changes due to the increase in the amount of $BaTiO_3$ This change is generally in the form of regional clusters and is not homogeneous. The presence of $BaTiO_3$ in PANI matrix led to increment in surface area, resulting in higher J_{sc} and FF value of the suggested DSSC. Moreover, increasing $BaTiO_3$ doping is clearly seen in the polymer matrix from SEM micrographs. The large amount of $BaTiO_3$ in PANI matrix led to agglomeration, resulting in decrement of surface area. Therefore, the optimum amount of dopant can be set as 1%.
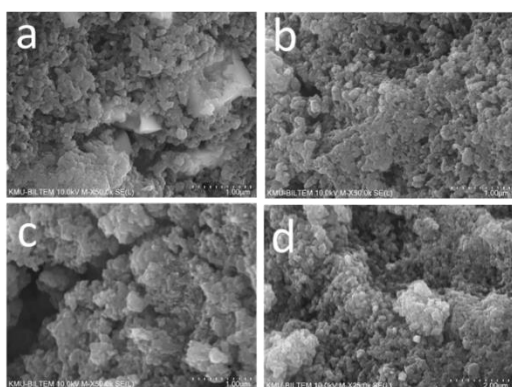
Figure 4. SEM of the a) SP, b) BP1, c) BP2 and d) BP3 nanocomposites.

Cyclic voltammetry (CV) measurements are generally an electrochemical measurement taken to examine the interaction of the counter electrode with the redox electrolyte used in DSSCs and the electrochemical kinetics of the counter electrode. The current density versus voltage graphs of the counter electrodes of the obtained PANI/$BaTiO_3$ composites are shown in Figure 5. CV plots of PANI-based counter electrodes typically show 2 distinct peaks, a pair of reduction-oxidation. A higher J_{red} value and a lower E_{pp} value indicate high electrocatalytic activity of the proposed counter electrode [22]. The value of the reduction peak current density (J_{red}) of the BP2 CE is slightly higher than that of the other CEs (Table 2). Compared to SP CE, the proposed BP2 CE structure provides extremely superior electrochemical stability and enhanced corrosion resistance.
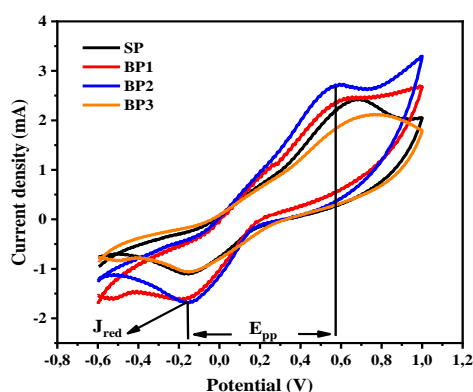

Figure 5. CV curves of SP, BP1, BP2, and BP3 polymers and composites

Table 2. Electrochemical parameters obtained from CV and EIS analysis of the counter electrodes.

Sample	J_{red} (mA)	E_{pp} (V)	R_s (ohm)	R_{ct} (ohm)	W (ohm)
SP	1.10	0.82	41	194	21
BP1	1.59	0.78	37	142	16
BP2	1.70	0.71	31	114	12
BP3	1.05	0.89	44	325	24

Electrochemical impedance spectroscopy (EIS) measurement is a powerful tool that provides very useful information and is used to examine the electron transfer kinetics occurring at interfaces [23, 24]. Therefore, EIS measurements of SP, BP1, BP2, and BP3 counter electrodes were carried out. Nyquist drawings of the EIS measurements taken are given in Figure 6. Equivalent circuit corresponding to Nyquist curves is given inside of Figure 6. R_s given in the circuit is the series resistance that is the first point where the high frequency first loop crosses the x-axis. R_{ct} is the electron transfer resistance that occurs at the opposite electrode/electrolyte interface. W (Warburg) is known as the diffusion impedance of the electrolyte on the CE surface. R_s, R_{ct}, and W values obtained by fitting Nyquist curves with the equivalent circuit are listed in Table 2. When Table 2 is examined, it is seen that R_s, R_{ct}, and W values decrease as a result of the effect of $BaTiO_3$ on the polymer structure. This indicates that the FTO/counter electrode and the counter electrode/electrolyte interfaces are improved, furthermore the diffusion of the electrolyte at the CE surface has improved [25-27].
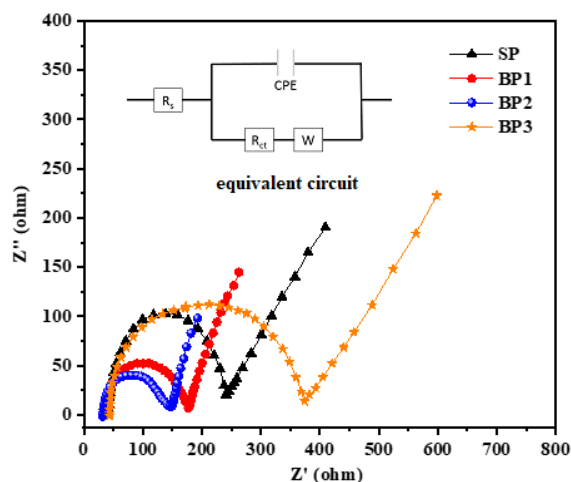
Figure 6. Nyquist plots of DSSCs based on SP, BP1, BP2, and BP3 counter electrodes.

J-V curves (Figure 7) were measured to evaluate the photovoltaic performance of the produced polymer and nanocomposite counter-electrode based DSSCs. Photovoltaic parameters obtained from J-V curves are displayed in Table 3. As can be seen from the table, it is seen that the FF and J_{sc} values of the BP2 cell have the highest values compared with the pure polymer and other composites. The FF and J_{sc} values of the BP2 cell were 62.5% and 14.56 mA / cm^2, respectively. The FF and J_{sc} values of the pure PANI (SP) cell were 55.4% and 12.10 mA/cm^2, respectively. As a result, the conversion efficiency increased from 4.58% to 6.37% with an increase of 39%. This improvement in efficiency can be

attributed to the increment of the J_{red} value from 1.10 to 1.70 mA/cm^2, the decrement of E_{pp} value from 0.82 to 0.71 V, and the lowering the R_s value from 41 to 31 Ω and R_{ct} value from 194 to 114 Ω, by incorporation of BaTiO₃ to PANI matrix.
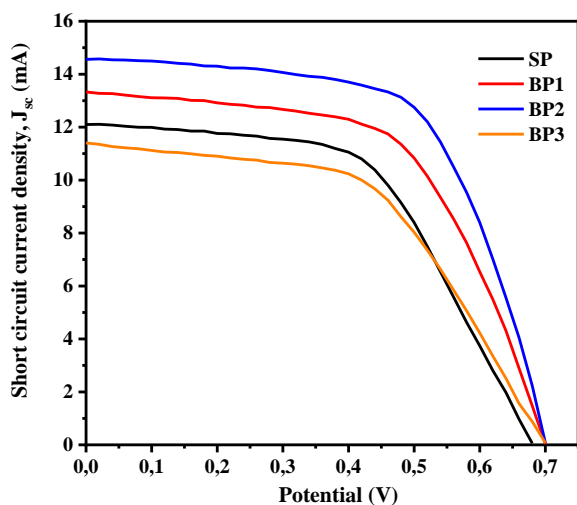

Figure 7. Current density vs. voltage plots of DSSCs based on SP, BP1, BP2, and BP3 counter electrodes.

Table 3. Photovoltaic parameters obtained from the J-V characterization of the solar cells.

Sample	J_{sc} (mA)	V_{oc} (V)	FF (%)	η (%)
SP	12.10	0.68	55.4	4.58
BP1	13.32	0.70	58.4	5.45
BP2	14.56	0.70	62.5	6.37
BP3	11.40	0.70	53.3	4.25

4 Conclusion

In this study, BaTiO₃ nano powders were obtained by microwave method and BaTiO₃/polymer composites were synthesized by chemical polymerization method by in situ method. Structural interaction parameters of all composite samples were performed by Fourier Transform Infrared Spectroscopy (FT-IR), Scanning Electron Microscope (SEM), X-Ray Diffractometer (XRD) and cyclic voltammetry (CV) analysis. In addition, the performance of composites as counter electrodes in dye sensitized solar cells (DSSC) was investigated in comparison pure PANI. From the XRD and FTIR results, it was determined that PANI/BaTiO₃ composites were synthesized successfully. It was used as a counter electrode in DSSCs to characterize the photovoltaic potentials of the produced nanocomposites. In photovoltaic analysis, the conversion efficiency of nanocomposite DSSCs increased by 39% compared to pure polymer counter electrode cells. By incorporation of BaTiO₃ to PANI, the charge transfer kinetics have been improved due to the improvement of electrical conductivity, electrocatalytic activity, as well as the interfacial states, and as a result, the conversion efficiency of the nanocomposite DSSCs has improved compared to the pure PANI counter electrode cells. Therefore, it can be said that produced nanocomposites can be used in DSSCs due to its low cost, high durability and performance instead of Pt, which is expensive and has limited stock.

Declaration

The authors declare that the ethics committee approval is not required for this study.

References

[1] Jangid, N. K., Jadoun, S., & Kaur, N. (2020). A review on high-throughput synthesis, deposition of thin films and properties of polyaniline. *European Polymer Journal*, 125, 109485.

[2] Maison, W., Kleeberg, R., Heimann, R. B., & Phanichphant, S. (2003). Phase content, tetragonality, and crystallite size of nanoscaled barium titanate synthesized by the catecholate process: effect of calcination temperature. Journal of the *European Ceramic Society,* 23(1), 127-132.

[3] Sengupta, L., & Sengupta, S. (1997). Novel ferroelectric materials for phased array antennas. *IEEE Transactions on ultrasonics, ferroelectrics, and frequency control,* 44(4), 792-797.

[4] Sengupta, L. C., Stowell, S., Ngo, E., O'day, M. E., & Lancto, R. (1995). Barium strontium titanate and non-ferroelectric oxide ceramic composites for use in phased array antennas. *Integrated Ferroelectrics,* 8(1-2), 77-88.

[5] Sönmezoğlu, S., Taş, R., Akın, S., & Can, M. (2012). Polyaniline micro-rods based heterojunction solar cell: structural and photovoltaic properties. *Applied Physics Letters*, 101(25), 253301.

[6] Kim, Y. H., Kim, M., Oh, S., Jung, H., Kim, Y., Yoon, T. S., ... & Ho Lee, H. (2012). Organic memory device with polyaniline nanoparticles embedded as charging elements. *Applied Physics Letters,* 100(16), 91.

[7] Mangal, S., Adhikari, S., & Banerji, P. (2009). Aluminum/polyaniline/GaAs metal-insulator-semiconductor solar cell: Effect of tunneling on device performance. A*pplied Physics Letters,* 94(22), 223509.

[8] Bousalem, S., Zeggai, F. Z., Baltach, H., & Benyoucef, A. (2020). Physical and electrochemical investigations on hybrid materials synthesized by polyaniline with various amounts of ZnO nanoparticle. *Chemical Physics Letters,* 741, 137095.

[9] Henshaw, G., Parkin, I. P., & Shaw, G. (1996). Convenient, low-energy synthesis of metal sulfides and selenides; PbE, Ag2E, ZnE, CdE (E= S, Se). *Chemical Communications*, (10), 1095-1096.

[10] Matteazzi, P., & Le Caër, G. (1992). Mechanically activated room temperature reduction of sulphides. *Materials Science and Engineering*: A, 156(2), 229-237.

[11] Biswas, S., Mondal, A., Mukherjee, D., & Pramanik, P. (1986). A chemical method for the deposition of bismuth sulfide thin films. *Journal of The Electrochemical Society*, 133(1), 48.

[12] Verma, A. K., & Rauchfuss, T. B. (1995). Chalcogenospecific Synthesis of 1, 2-Se2S6 Using ZnS6 (TMEDA). *Inorganic Chemistry*, 34(24), 6199-6201.

[13] S.H. Yu, J. Yang, Y.S. Wu, Z.H. Han, Y. Xie, Y.T. Qian, Hydrothermal preparation and characterization of rod-like ultrafine powders of bismuth sulfide, Mater Res Bull 33(11) (1998) 1661-1666.

[14] Yu, S. H., Yang, J., Wu, Y. S., Han, Z. H., Xie, Y., & Qian, Y. T. (1998). Hydrothermal preparation and characterization of rod-like ultrafine powders of bismuth sulfide. *Materials research bulletin,* 33(11), 1661-1666.

[15] J.J. Zhu, S.W. Liu, O. Palchik, Y. Koltypin, A. Gedanken, A novel sonochemical method for the preparation of nanophasic sulfides: Synthesis of HgS and PbS nanoparticles, Journal of Solid State Chemistry 153(2) (2000) 342-348.

[16] Zhu, J., Liu, S., Palchik, O., Koltypin, Y., & Gedanken, A. (2000). A novel sonochemical method for the preparation of nanophasic sulfides: synthesis of HgS and PbS nanoparticles. *Journal of Solid State Chemistry,* 153(2), 342-348.

[17] Wang, K. L., Zhang, Q. B., Sun, M. L., Wei, X. G., & Zhu, Y. M. (2001). Rare earth elements modification of laser-clad nickel-based alloy coatings. *Applied surface science,* 174(3-4), 191-200.

[18] Xiao, S., Li, X., Sun, W., Guan, B., & Wang, Y. (2016). General and facile synthesis of metal sulfide nanostructures: In situ microwave synthesis and application as binder-free cathode for Li-ion batteries. *Chemical Engineering Journal,* 306, 251-259.

[19] Luo, F., Li, J., Yuan, H., & Xiao, D. (2014). Rapid synthesis of three-dimensional flower-like cobalt sulfide hierarchitectures by microwave assisted heating method for high-performance supercapacitors. *Electrochimica Acta,* 123, 183-189.

[20] Taş, R., Gülen, M., Can, M., & Sönmezoğlu, S. (2016). Effects of solvent and copper-doping on polyaniline conducting polymer and its application as a counter electrode for efficient and cost-effective dye-sensitized solar cells. *Synthetic Metals,* 212, 75-83.

[21] Taş, R., Can, M., & Sönmezoğlu, S. (2015). Preparation and characterization of polyaniline microrods synthesized by using dodecylbenzene sulfonic acid and periodic acid. *Turkish Journal of Chemistry*, 39(3), 589-599.

[22] Zheng, X., Deng, J., Wang, N., Deng, D., Zhang, W. H., Bao, X., & Li, C. (2014). Podlike N-doped carbon nanotubes encapsulating FeNi alloy nanoparticles: high-performance counter electrode materials for dye-sensitized solar cells. *Angewandte Chemie International Edition*, 53(27), 7023-7027.

[23] Xia, J., Chen, L., & Yanagida, S. (2011). Application of polypyrrole as a counter electrode for a dye-sensitized solar cell. *Journal of Materials Chemistry*, 21(12), 4644-4649.

[24] Zhang, X., Liu, J., Li, S., Tan, X., Zhang, J., Yu, M., & Zhao, M. (2013). DNA assembled single-walled carbon nanotube nanocomposites for high efficiency dye-sensitized solar cells. *Journal of Materials Chemistry A,* 1(36), 11070-11077.

[25] Wu, J., Yue, G., Xiao, Y., Huang, M., Lin, J., Fan, L., ... & Lin, J. Y. (2012). Glucose aided preparation of tungsten sulfide/multi-wall carbon nanotube hybrid and use as counter electrode in dye-sensitized solar cells. A*CS applied materials & interfaces,* 4(12), 6530-6536.

[26] Qiu, L., Jiang, Y., Sun, X., Liu, X., & Peng, H. (2014). Surface-nanostructured cactus-like carbon microspheres for efficient photovoltaic devices. *Journal of Materials Chemistry A,* 2(36), 15132-15138.

[27] Wei, W., Wang, H., & Hu, Y. H. (2014). A review on PEDOT-based counter electrodes for dye-sensitized solar cells. *International Journal of Energy Research,* 38(9), 1099-1111.